Inkjet Printed Single Layer High-Density Circuitry for a MEMS Device

Mika-Matti Laurila, Ayat Soltani, Matti Mäntysalo
Tampere University of Technology
Korkeakoulunkatu 10, 33720 Tampere, Finland
mika-matti.laurila@tut.fi, +358 50 301 4394

Abstract

For example high-density redistribution layers (RDL) require narrow conductor width and low enough resistance. We have studied the applicability of an additive electrodynamic inkjet printer, Super Inkjet (SIJ), as a potential replacement for the current non-additive manufacturing method used in circuitry fabrication for MEMS devices. This was done by examining the topography of the printed lines and relating this to the resistance. For example five and two micron wide conductors were demonstrated with aspect ratio as high as 0,8 and 0,9. The average resistivity value for the five micron wide conductors was 17 µOhm·cm and 15 µOhm·cm for the two micron case. Also the repeatability of the line width calibration process was evaluated. The accuracy was found to be approximately one micron.

Introduction

Printed electronics is one of today's revolutionary innovations to fabricate electronics. It offers a cost-effective, more sustainable manufacturing method for flexible displays [1], photovoltaics [2], sensors [3], antennas [4], supercapacitors [5], and transistors [6]. Inkjet printing is an additive, contactless, and digital manufacturing method which uses a direct deposition of functional materials on various substrates to create conductive, semi-conductive or dielectric structures. The non-contact nature of the deposition enables printing on substrates with varying stiffness and surface topography, whereas the digital nature of the fabrication process enables personalization of products with minimal idle time between the current product and the next. This increases the agility of the manufacturing process. The cost efficiency is increased by scaling and the additive nature of the process because less material is used; the environment benefits from this as well. [7]

Narrow high-density lines are needed for interconnections and in particular RDLs. The most obvious way to minimize the feature size is to decrease the size of the droplet. In conventional inkjet technologies this is done by decreasing the nozzle diameter. However, this increases the forces necessary for droplet ejection and introduces a narrow processing window with applicable surface tension and viscosity of ink. Therefore, other techniques like increasing the substrate temperature [8], predefining surface energies [9], fluid assisted de-wetting [10], and advanced printing algorithms [11] have been developed. A line width of 25-50 µm can be achieved using the conventional techniques. So far inkjet printed nano-metal particles have been used to make connections between the chips and printed circuit boards (e.g. Chip-on-Board) [12] as well as between the chips and the package (e.g. System-in-Package) [13]. [7]

The limiting factor in incorporating conventional inkjet technologies to the electronics packaging is the relatively large line width. In this article, we investigate the use of a novel type of technology, namely the electrodynamic inkjet, as an alternative fabrication method for a high-density re-distribution layer (RDL) of a MEMS device. The used printer was a Super Inkjet (SIJ) capable of sub-femtoliter droplets enabling line widths of only few microns [14]. Because of the minuscule volume of each droplet, the printed patterns will be very thin as well as narrow. This means that in order to achieve an appropriate resistance, multiple layers have to be printed. Thus, the layer count – resistance relationship has to be investigated. The line width calibration accuracy has to be analyzed as well since it will affect the minimum conductor-to-conductor distance or line density.

This article will analyze the aforementioned aspects of the SIJ printed conductors for two different line widths, 5 and 2 microns, and evaluate the applicability of SIJ for manufacturing a high density RDL by investigating the stability of the process.

Materials and methods

The ink used in this research was commercial Harima NPS-J [15] supplied by Harima Chemicals Group which contains silver nanoparticles capped with polymer to prevent agglomeration; these are dispersed in tetradecane solvent. The recommended sintering time and temperature are 1h and 220 °C, solid content is 65 wt% and resistivity 3 µOhm·cm. To avoid possible agglomerations and clogging of the nozzle the ink was filtered before use with 0.2 micron GHP membrane filter. The ink parameters can be found from Table 1.

Table 1. Harima NPS-J parameters [15]

Parameter	Value
Particle size	~12 nm
Solid content	65 wt%
Sintering condition	220°C for 60 min
Resistivity	3 µOhm·cm
Viscosity	9 mPas·s
Thickness shrinkage rate	83 %

The substrate was a silicon wafer with a two micron silicon oxide layer on top. The wafers were provided by Murata Electronics Finland Oy. Before printing the wafers were wiped with isopropanol and cleaned with oxygen-plasma using the following parameters: O2 flow 2 sccm, pressure 100 mTorr, RF power 100 W for duration of ten

minutes; the equipment was Plasmalab System 100 from Oxford Insturments.

The test patterns were printed using the Super Inkjet printer shown in Figure 1 and developed by SIJ Technology Inc., Japan. Unlike the piezoelectric or thermal actuator based conventional inkjet technologies, the SIJ creates an oscillating electric field between the substrate plate and the ink reservoir (nozzle) by charging the ink. With optimized parameter settings this enables generation of femtoliter sized droplets from the nozzle tip. The parameters include for example the value, waveform and the frequency of the voltage applied between the nozzle and the substrate, the printing speed and the nozzle-to-substrate distance. The nozzle type can be changed as well; because of the small line widths, the Super Fine nozzle was used. With less than two microns, it has the smallest nozzle diameter of the three options.

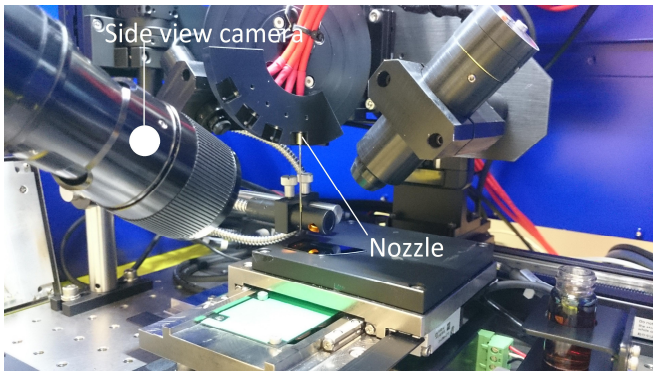

Figure 1. Super Inkjet developed by SIJ Technology, Japan. The nozzle type is the Super Fine nozzle.

Line width was calibrated with a zig-zag pattern shown in Figure 2a before printing four point test structure shown in Figure 2b. The calibration was done visually by using the side view camera marked in Figure 1 and printing the aforementioned zig-zag pattern with a conductor-to-conductor distance few microns larger than the desired line width. For Test A (five micron desired line width) the conductor-to-conductor distance was eight microns; for the Test B (two micron case), five microns was used. During the line width calibration the frequency (f), speed of the substrate (v), waveform (wf) and nozzle-to-substrate distance (d) were kept constant while the environmental parameters such as humidity (h) and temperature (T) were kept as constant as possible. Before printing the zig-zag pattern the nozzle is purged with an overvoltage (Vpurge) which forces the ink out of the nozzle thus getting rid of the possible dried up ink which might clog the nozzle. The bias voltage level (Vbias) and amplitude of the voltage (Vamp) are very high at the start of the zig-zag pattern producing a line with larger width than the pitch of the structure. During printing Vbias and Vamp are reduced to make the line width narrower. When the subsequent lines can be seen as separate from the side view camera, the line width should be in the right range. The parameter values at this point are shown in Table 2 for Test A and Test B structures.

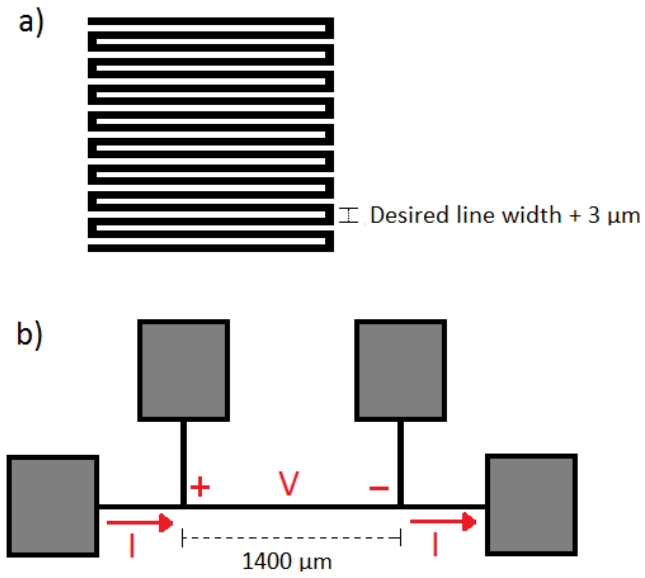

Figure 2. a) Zig-zag pattern for line width determination; b) 4 point pattern used for resistance measurements. The structures haven't been drawn to scale. After calibrating the line width with (a) the printing proceeds to the actual test structure (b). The pads (grey) were printed with Dimatix material printer.

Table 2. Printing parameters for 5 micron and 2 micron test structures.

Parameter	Test A (5 micron width)	Test B (2 micron width)
Number of sets	2	1
Number of layers	1-10, 15, 20, 25, 30, 35, 40	10, 15, 20, 25, 30, 35, 40
Vbias (V)	170	160
Vmax (V)	200	186
wf	sinusoidal	sinusoidal
f (Hz)	1000	1000
v (mm/s)	1	1
Vpurge (V)	1000	1000
d (microns)	~30 microns	~30 microns
H (%)	40…50	40…50
T (C)	21,4	22,6

After the goal line width is achieved the printing moves directly to the actual test structure. For resistance measurements this meant a four point structure shown in Figure 2b with the actual measurement setup shown in Figure 3. In Test A two sets were printed with 1, 2, 3, 4, 5, 6, 7, 8, 9, 10, 15, 20, 25, 30, 35 and 40 layers. In Test B only one set was printed with 10, 15, 20, 25, 30, 35 and 40 layers. To make the process faster, the contact pads were printed with Dimatix material printer (DMP-2831) using the same ink.

After printing, the samples were sintered for 1 hour in an oven heated to 220 °C.

The topography of the conductors was measured with an atomic force microscope XE-100, made by Park Systems Corp. The sample pictures were taken from random places along the conductors; the picture size was 10x10 microns. The topography of the sample measurements was analyzed with the image analysis tool XEI, also by Park Systems Corp. The sample length was deemed large enough by measuring some of the conductors from different regions and comparing the measurements with each other.

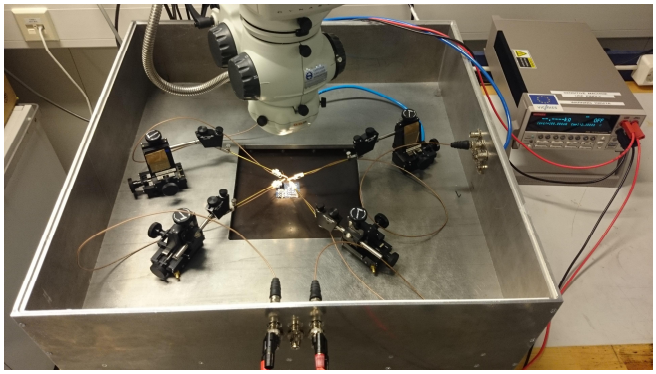

Figure 3. Measurement setup with Keithley 2400 multimeter and probe station

The resistances of sintered samples were measured using a Keithley 2400 multimeter and a purpose built probe station; see Figure 3 for the measurement setup. In the four point resistance measurement current is fed through the conductor and voltage drop along the length of the conductor is measured (see Figure 2b.).

Results and analysis

The number of layers required for reasonable resistance value increases as the conductor width decreases: since the cross-sectional area of the conductor must remain the same, thickness of the narrow conductor has to be increased relative to the wide conductor. In other words, the aspect ratio of the narrow conductor has to be higher than the aspect ratio of a wide conductor to get an equal resistance. This means that multiple layers have to be printed. Although it sounds like a major drawback when considering the processing time, the problem is relieved by the fact that the evaporation rate increases as the droplet size decreases. With conventional inkjet technologies there has to be a certain amount of time delay between consecutive layers to allow the previous layer to dry up [16], but in the case of very small droplets this time delay will be significantly reduced or even non-existent [17] allowing quick build-up of high aspect ratio conductors. All the conductors in this report were printed without time delay between subsequent layers.

Figure 4 consists of enhanced color AFM images of Test A showing how the appearance of the conductors change as the number of layers is increased from 1 (a), 5 (b), 10 (c) to 15 layers (d).

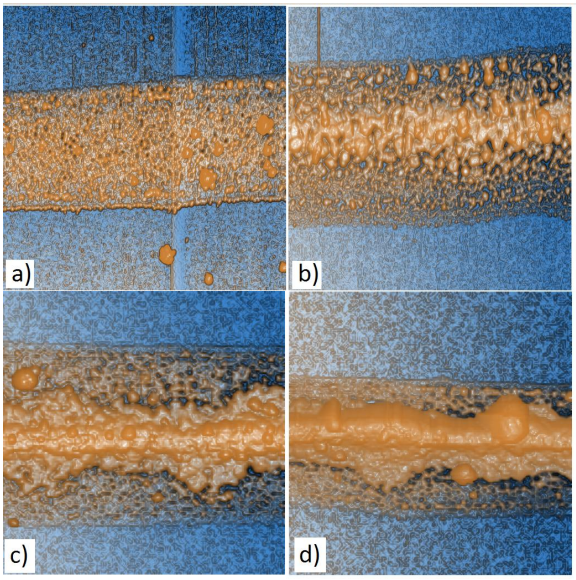

Figure 4. Enhanced color AFM images of a) 1 layer, b) 5 layer, c) 10 layer and d) 15 layer sintered conductors for 5 micron line width. Note that the picture (b) has 7x10 micron (height x width) dimension instead of 10x10 microns.

As expected, the individual layers are very thin. It also seems to be that the first few layers act as a kind of seed layer for the subsequent ones; when the layer number is increased the additional ink starts to accumulate to the middle of the conductor. This can be clearly seen in Figure 5, which consists of average topographical graphs of the samples shown in Figure 4. Similar behavior was observed by Sadie et al. for pillar structures fabricated with conventional inkjet. They divided the pillar formation in three regimes: wetting, tapering and growth. Similar growth mechanism could explain the growth of the SIJ printed lines as well. See reference [16] for more detailed analysis.

The average peak to valley heights for the curves shown in Figure 5 are 50 nm, 183 nm, 570 nm and 850 nm for the samples (a), (b), (c) and (d), respectively. It is interesting to note, that the average peak to valley height of the one layer sample is about one third of the sample with five layers. If the jetting rate would be the same in both cases, one would expect the average peak to valley height to increase in 50 nanometer increments - or even larger, if it is assumed that the ink starts to accumulate to the middle of the conductor after sufficient number of layers. Because this kind of dependency is not detected, the only viable explanation is that the jetting rate (ink flow rate) changes during fabrication process.

From Figure 5 it can be seen that there is also another type of process variation, namely that of the line width. To test the accuracy of the line width calibration a sample set of 11 structures was measured from an earlier test run where the desired line width was also five microns. The results showed that the achieved line width is most likely smaller than the desired one with few exceptions. The standard deviation for the error was 1 micron or 20% of the desired line width. From the high density circuitry point of view this is good

news since the structures will rarely short circuit because of too wide conductors.

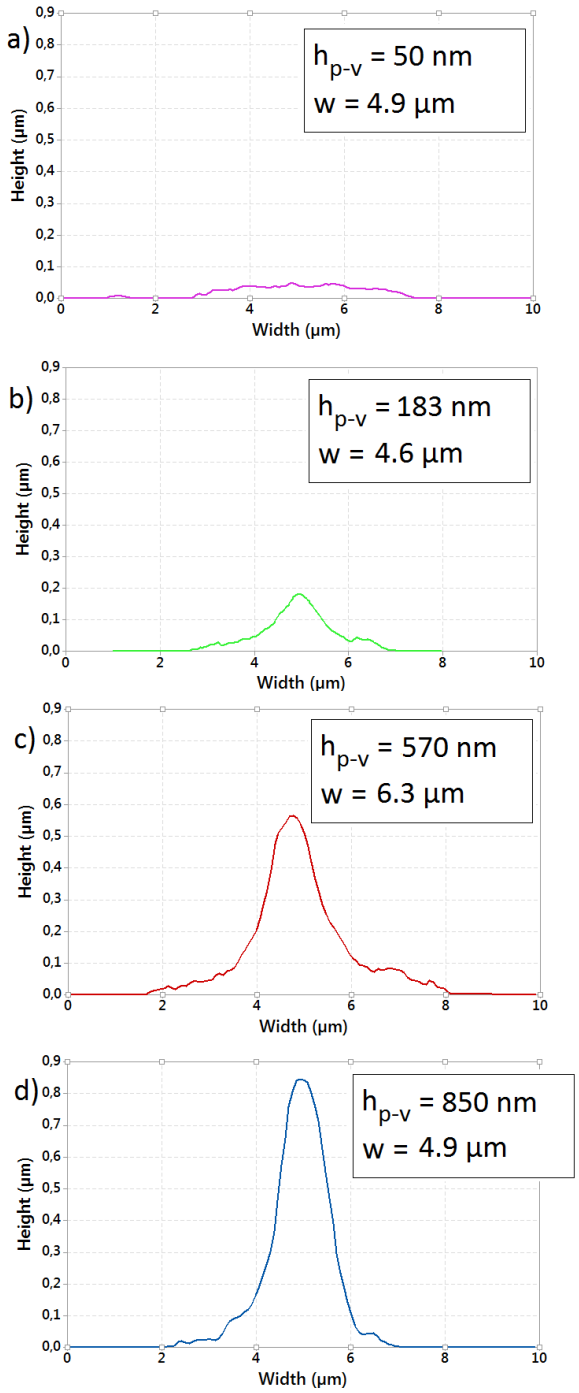

Figure 5. Average topography of samples in Figure 4: a) 1 layer, b) 5 layer, c) 10 layer and d) 15 layer. h(p-v) stands for peak-to-valley height and w for width.

The calibration error seems to be important since it affects the minimum conductor-to-conductor distance. If the standard deviation of the calibration error is used as a guide value, the conductor-to-conductor distance should be at least 1 micron. But the line width and conductor width are not necessarily equal in the case of SIJ. As mentioned earlier, the first few layers are very thin - actually so thin that they do not conduct at all. This can be seen from the graph of Figure 6 which shows the relation of the layer number to the sheet resistance for the Set 1 and Set 2 of Test A and Test B. This means that it might be possible to place the conductors so close to each other that the first layers touch without short circuiting the structure thus increasing the density of the parallel signal paths.

From Figure 6 it is clear that similar relationship between the layer number and thickness applies for the conductors of both Tests, A and B (2 micron). The decrease in sheet resistance starts to flatten out at approximately 25 to 30 layers. This behavior is as expected since the sheet resistance equals resistivity divided by thickness. Thus, it can be concluded that the conductors in the RDL should have around 30 layers regardless of the conductor width; this number seems to give the optimum combination of processing time and sheet resistance.

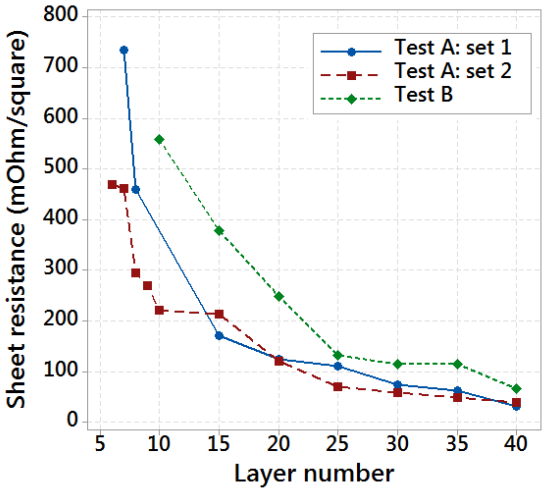

Figure 6. The sheet resistance – layer number relationship for the Test A. Sheet resistance is shown in mOhms/square.

To compare the resistivity values to the value provided by the ink manufacturer (see Table 1), the conductor thicknesses were measured for the four conductors with the highest layer count (15 to 40) and the resistivity calculated based on this. The average resistivity value for the Test A was 17 µOhm·cm and 15 µOhm·cm for the Test B. The deviation from the ink datasheet value of 3 µOhm·cm could be explained by the somewhat unusual topography of the conductors printed with electrodynamic printer. The sheet resistance works best for conductors with approximately rectangular profile, but as shown in Figure 5, the profile of the current conductors is shaped like a bell curve. It is also probable that a substantial part of the line is non-conductive, the conductivity taking place in the center where most material is accumulated instead of the edges with less material; see Figure 4. Because

the measured line width takes account of this non-conductive part as well, the resulting sheet resistance values are higher than the true value. This would also increase the resistivity, which is calculated based on the sheet resistance.

Conclusions

General topography of the SIJ printed conductors was investigated for two line widths, five micron and two micron. It was found out that multiple layers are needed to achieve low sheet resistance with approximately 30 layers producing the optimum combination of resistance and process time. The resistivity of the conductors was 15 to 17 µOhm·cm, approximately ten times higher than the resistivity of bulk silver. The line width calibration accuracy was investigated as well: in most cases narrower-than-intended line widths were produced; the standard deviation of the error was one micron. The conductor resistivity was found out to be approximately five times higher than the datasheet value.

Acknowledgments

This work is supported by ENIAC-JU Project Prominent grant No. 324189 and Tekes grant No. 40336/12.

The authors would like to acknowledge Murata Electronics Finland who provided the wafers used in the tests.

The authors would also like to thank M.Sc. Maiju Hiltunen for patient guidance with the use of the AFM.

References

1. B. Yoon et al, “Inkjet Printing of Conjugated Polymer Precursors on Paper Substrate for Colorimetric Sensing and Flexible Electrothermochromic Display”, *Advanced Materials*, vol. 23, no. 46, pp. 5492-5497, Dec. 2011.
2. S. H. Eorn et al, “Polymer Solar Cells Based On Inkjet-Printed PEDOT:PSS layer”, *Organic Electronics*, vol. 10, no. 3, May. pp. 536-542, 2009.
3. V. Dua et al, “All-Organic Vapor Sensor Using Inkjet-Printed Reduced Graphene Oxide”, *Angewandte Chemie International Edition*, vol. 49, no. 12, pp. 2154-2157, Mar. 2010
4. M. Mäntysalo et al, “An Inkjet-Deposited Antenna for 2.4 GHz applications”, *AEU – International Journal of Electronics and Communications*, vol. 63, no. 1, pp. 31-35, Jan. 2009
5. D. Pech et al, “Elaboration of a Inkjet-Printed Carbon Electrochemical Capacitor”, *Journal of Power Sources*, vol. 195, no. 4, pp. 1266-1269, Feb. 2010
6. H. Sirringhaus et al, “High-Resolution Inkjet Printing of All-Polymer Transistor Circuits”, *Science*, vol. 290, no. 5499, pp. 2123-2126, Dec. 2000
7. I. M. Hutchings and G. D. Martin, “Chapter 1: Introduction to Inkjet Printing for Manufacturing” and “Chapter 2: Fundamentals of Inkjet Technology”, I. M. Hutchings and G. D. Martin, *Inkjet Technology for Digital Fabrication*, John Wiley & Sons Ltd, Chichester, UK
8. D. Soltman et al, “Inkjet-Printed Line Morphologies and Temperature Control of the Coffee Ring Effect”, *Langmuir*, Vol. 24, no. 5, pp. 2224-2231, Jan. 2008
9. J. Z. Wang et al, “Dewetting of conducting polymer inkjet droplets on patterned surfaces”, *Nature Materials*, vol. 3, pp. 171-176, Feb. 2004
10. C.P.R. Dockendorf et al, “Size reduction of nanoparticle ink patterns by fluid-assisted dewetting”, vol. 88, no. 13, March 2006
11. Mäntysalo, M., Mansikkamäki, P., “Inkjet Deposited Interconnections for Electronic Packaging”, Proceedings of IST Digital Fabrication, Alaska, USA, Sept. 16th-21st, 2007, pp. 813 817.
12. Santtu Koskinen, Lasse Pykäri, Matti Mäntysalo, ”Electrical Performance Characterization of an Inkjet-Printed Flexible Circuit in a Mobile Application”, IEEE Transaction on Components, Packaging and Manufacturing Technology, Vol. 3, no. 9, 2013, pp. 1604 – 1610.
13. Miettinen et al, “Inkjet printed System-in-Package design and manufacturing”, *Microelectronics Journal*, vol. 39, no. 12, pp. 1740-1750, Dec. 2008
14. N. Shirakawa et al. “Fine Pitch Copper Wiring Formed with Super-Inkjet and the Oxygen Pump”, *Japanese Journal of Applied Physics*, Vol. 52, no. 5S1, 2013
15. Harima Chemicals Group, “Nano Paste Series – Datasheet”, https://www.harima.co.jp/en/products/electronics/pdf/brochure14e_21.pdf
16. J. A. Sadie et al, “Three-dimensional inkjet-printed interconnects using functional metallic nanoparticle inks”, *Advanced Functional Materials*, vol. 24, no. 43, pp. 6834-6842, Nov. 2014
17. C. C. Ho et al, “A Super Ink Jet Printed Zinc-Silver 3D Microbattery”, *Proceedings of PowerMEMS 2008*, Sendai, Japan, Nov. 2008